

## ORIGINAL ARTICLE

# A *Drosophila* model system to assess the function of human monogenic podocyte mutations that cause nephrotic syndrome

Yulong Fu<sup>1,†</sup>, Jun-yi Zhu<sup>1,†</sup>, Adam Richman<sup>1</sup>, Zhazheng Zhao<sup>2</sup>, Fujian Zhang<sup>3</sup>, Patricio E. Ray<sup>4,5</sup> and Zhe Han<sup>1,5,\*</sup>

<sup>1</sup>Center for Cancer and Immunology Research, Children's National Health Systems, 111 Michigan Ave. NW, Washington, DC, USA, <sup>2</sup>Department of Nephrology, First Affiliated Hospital of Zhengzhou University, Zhengzhou, People's Republic of China, <sup>3</sup>Division of Nephrology, Nanfang Hospital, Southern Medical University, Guangzhou, People's Republic of China, <sup>4</sup>Center for Genetic Medicine Research, Children's National Health Systems, 111 Michigan Ave. NW, Washington, DC, USA and <sup>5</sup>Department of Pediatrics, The George Washington University School of Medicine and Health Sciences, Washington, DC, USA

\*To whom correspondence should be addressed at: Children's Research Institute, Children's National Health System, 111 Michigan Ave. NW, Washington, DC 20010, USA. Tel: +202 476 2528; Fax: +202 476 6498; Email: zhan@childrensnational.org

## Abstract

Many genetic mutations have been identified as monogenic causes of nephrotic syndrome (NS), but important knowledge gaps exist in the roles of these genes in kidney cell biology and renal diseases. More animal models are needed to assess the functions of these genes *in vivo*, and to determine how they cause NS in a timely manner. *Drosophila* nephrocytes and human podocytes share striking similarities, but to what degree these known NS genes play conserved roles in nephrocytes remains unknown. Here we systematically studied 40 genes associated with NS, including 7 that have not previously been analysed for renal function in an animal model. We found that 85% of these genes are required for nephrocyte functions, suggesting that a majority of human genes known to be associated with NS play conserved roles in renal function from flies to humans. To investigate functional conservation in more detail, we focused on *Cindr*, the fly homolog of the human NS gene *CD2AP*. Silencing *Cindr* in nephrocytes led to dramatic nephrocyte functional impairment and shortened life span, as well as collapse of nephrocyte lacunar channels and effacement of nephrocyte slit diaphragms. These phenotypes could be rescued by expression of a wild-type human *CD2AP* gene, but not a mutant allele derived from a patient with *CD2AP*-associated NS. We conclude that the *Drosophila* nephrocyte can be used to elucidate clinically relevant molecular mechanisms underlying the pathogenesis of most monogenic forms of NS, and to efficiently generate personalized *in vivo* models of genetic renal diseases bearing patient-specific mutations.

## Introduction

Advances in genomic analysis techniques have enabled the identification of a large number of genes, encoding products

with diverse functions, that when mutated contribute to nephrotic syndrome (NS). Many cases of chronic kidney diseases (CKD) are associated with single gene mutations that affect the

<sup>†</sup>The authors wish it to be known that, in their opinion, the first 2 authors should be regarded as joint First Authors.

Received: October 22, 2016. Revised: December 8, 2016. Accepted: December 16, 2016

© The Author 2017. Published by Oxford University Press. All rights reserved. For Permissions, please email: journals.permissions@oup.com

function of podocytes (1–5). These studies point to podocytes as a key renal target to precipitate CKD (6–9). For example, among patients with steroid-resistant nephrotic syndrome, several mutations have been found in podocyte genes that affect the structure and function of the slit diaphragm (SD), the regulation of the actin cytoskeleton proteins, basement membrane components, cell membrane, adhesion molecules, mitochondrial function, endocytosis, cation flux, Coenzyme Q10 biosynthesis, and the regulation of transcription (10–20). Our understanding of the molecular and cellular mechanisms underlying renal pathologies caused by these mutations, and our potential to develop new therapeutic treatment approaches based on that knowledge, have to date largely come from experimental studies performed in the mouse and zebrafish models. Although a relatively simple animal model system, *Drosophila* is unrivalled with respect to the abundance of highly sophisticated genetic approaches and well-established, available resources that can be exploited to rapidly and efficiently investigate specific

molecular pathways and cellular targets implicated in abnormal cell physiologies relevant to disease (12,21–26). *Drosophila* can thus be used as a high-throughput experimental disease-model platform, to validate the large amount of data generated from clinical genomics.

Overall, 75% of human disease associated genes are represented in the *Drosophila* genome by functional homologs (27,28). We have developed a fly model to investigate genetic, molecular, and cellular targets of cell injury in *Drosophila* nephrocytes, that is relevant to human podocytes (12,26,29,30), and provides new *in vivo* information to complement the excellent studies done in mice. Briefly, the *Drosophila* pericardial nephrocyte (hereafter, nephrocyte) is remarkably similar, both structurally and functionally, to the mammalian podocyte (Fig. 1A–C) (24,25,31,32). Nephrocytes are relatively large cells positioned beside the dorsal vessel (the fly heart). The dorsal vessel, by regular contractions, maintains hemolymph (insect blood) circulation throughout the body cavity. The nephrocytes carry out

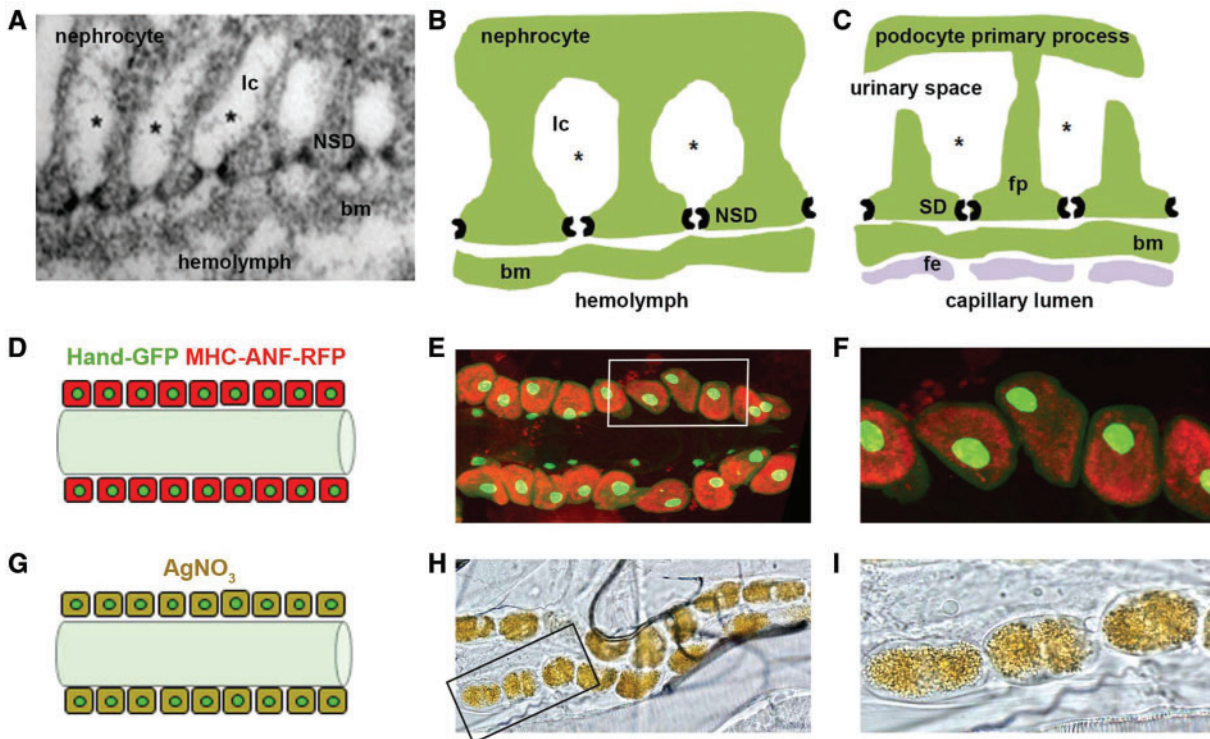


**Figure 1.** Comparison of nephrocyte and podocyte basic features, and nephrocyte functional assays. (A–C). Insect nephrocytes and mammalian podocytes are structurally and functionally homologous. Panel A is a transmission electron micrograph of a *Drosophila* nephrocyte. Panels B and C compare structural and functional features of nephrocytes and podocytes, respectively. A basement membrane (bm) interposes a size and charge selective filtration barrier between the nephrocyte slit diaphragm (NSD) and the hemolymph of the insect open circulatory system, and the podocyte slit diaphragm (SD) and blood from the mammalian capillary lumen. In the latter case blood encounters the bm after exiting the capillary lumen through a fenestrated endothelial (fe) cell layer. The principal cellular structure in nephrocytes and podocytes mediating filtration is a slit diaphragm. In podocytes, SD proteins form intercellular filtration barriers between adjacent foot processes (fp), the intercalating termini of primary processes originating from different podocyte cells. In nephrocytes, NSD proteins form intracellular filtration barriers on either side of lacunar channel (lc) openings. In nephrocytes, filtered low molecular weight molecules (represented by \*) are reabsorbed by endocytosis from the lacunar channel membrane. In podocytes the ultrafiltrate passing through the SD enters the urinary space, and is subsequently reabsorbed by proximal tubule cells. The nephrocyte therefore bears striking similarities not only to the mammalian podocyte, but is functionally homologous to proximal tubule cells as well. (D–F). Functional assay measuring nephrocyte uptake of hemolymph protein. Panel D is a schematic diagram showing pericardial nephrocytes aligned on either side of the heart tube. In this assay, muscle cells (not shown) express a MHC-ANF-RFP transgene in which a myosin heavy chain (MHC) promoter directs expression of an atrial natriuretic peptide (42) - red fluorescent protein (RFP) fusion protein. ANF-RFP is secreted into the fly hemolymph, from which it is filtered and endocytosed by nephrocytes leading to cytoplasmic red fluorescence. Hand-GFP transgene expression is visualized as green fluorescence concentrated in the nuclei of nephrocytes (shown) and cardiomyocytes (not shown). Panel E shows RFP fluorescence (54) in the cytoplasm of adult nephrocytes, reflecting endocytosis of ANF-RFP fusion protein filtered from the hemolymph. Cardiomyocytes lack red fluorescence. Green fluorescence in nephrocyte and cardiomyocyte nuclei is due to Hand-GFP expression. Panel F is a higher magnification image of cells (boxed) from panel E. (G–I). Functional assay measuring nephrocyte uptake of  $\text{AgNO}_3$ . Panel G is a schematic diagram showing pericardial nephrocytes containing endocytosed and sequestered  $\text{AgNO}_3$ . Panel H is a photomicrograph showing ingested  $\text{AgNO}_3$  sequestered in larval nephrocytes. Panel I is a higher magnification image of cells (boxed) from panel H.

**Table 1.** Human monogenic Nephrotic Syndrome (NS) genes and their *Drosophila* orthologs

| Human Gene | <i>Drosophila</i> Ortholog | Function                           | Cellular Localization | Renal Pathology |
|------------|----------------------------|------------------------------------|-----------------------|-----------------|
| NPHS1      | Sns                        | Filtration                         | SD                    | SRNS            |
| NPHS2      | Mec2                       | Linker                             |                       | SRNS            |
| CD2AP      | Cindr                      | Adaptor protein                    |                       | SRNS            |
| PTPRO      | Ptp10D                     | Receptor-type tyrosine phosphatase |                       | SRNS            |
| TRPC6      | Trpgamma                   | Calcium channel                    |                       | SRNS            |
| MYH9       | Zip                        | Myosin motor                       | Actin Cytoskeleton    | SRNS            |
| MYO1E      | Myo61F                     |                                    |                       | SRNS            |
| ACTN4      | Actn                       | Actin binding                      |                       | SRNS            |
| INF2       | Form3                      |                                    |                       | SRNS            |
| SYNPO      | CG1674                     |                                    |                       | NS              |
| ANLN       | Scra                       |                                    |                       | SRNS            |
| KANK1      | Kank                       | Actin regulation                   |                       | SRNS            |
| KANK2      |                            |                                    |                       | SRNS            |
| KANK4      |                            |                                    |                       | SRNS            |
| ARHGAP24   | RhoGAP92B                  | Signaling                          |                       | SRNS            |
| ARHGDI     | RhoGDI                     |                                    |                       | SRNS            |
| LMX1B      | CG32105                    | Transcription factor               | Nucleus               | SRNS            |
| SMARCAL1   | Marcal1                    |                                    |                       | SRNS            |
| PAX2       | Sv                         |                                    |                       | NS              |
| E2F3       | E2f                        |                                    |                       | NS              |
| NXF5       | Sbr                        | RNA export                         |                       | NS              |
| ZMPSTE24   | Ste24a                     | Lamin A processing                 |                       | NS              |
| LMNA       | Lam                        | Lamina                             |                       | NS              |
| CUBN       | Cubn                       | Endocytosis                        | Plasma membrane       | IGS             |
| AMN        | Amn                        |                                    |                       | IGS             |
| SCARB2     | Emp                        | Proteolysis                        | Lysosome              | SRNS            |
| PMM2       | CG10688                    | Glycosylation                      | Cytosol               | NS              |
| ALG1       | CG18012                    |                                    | ER                    | NS              |
| COQ2       | Coq2                       | Coenzyme Q synthesis               | Mitochondrion         | SRNS            |
| COQ6       | CG7277                     |                                    |                       | SRNS            |
| PDSS2      | CG10585                    |                                    |                       | SRNS            |
| ADCK4      | CG32649                    |                                    |                       | SRNS            |
| GPC5       | Dally                      | Signaling                          | Plasma membrane       | NS              |
| ITGA3      | Mew                        | Adhesion                           |                       | SRNS            |
| ITGB4      | Mys                        |                                    |                       | SRNS            |
| CD151      | Tsp74F                     |                                    |                       | NS              |
| LAMB2      | LanB1                      | GBM Structure                      | ECM                   | SRNS            |
| COL4A3     | Col4a1                     |                                    |                       | Alport          |
| COL4A4     |                            |                                    |                       | Alport          |
| COL4A5     |                            |                                    |                       | Alport          |

hemolymph filtration and reabsorption functions homologous to mammalian podocytes and proximal tubule cells, respectively, by virtue of nephrocyte slit diaphragms (NSD) spanning the equivalents of foot processes and lacunar channels that expand the plasma membrane area to increase uptake of filtered hemolymph components (24,25,29). Nephrocytes are so positioned that filtered hemolymph enters the dorsal vessel for redistribution.

Analysing the available literature up to the end of 2015, we identified 40 genes that are directly associated with NS and have clear *Drosophila* homologs with available RNAi targeting fly lines (33–36). We carried out this study to explore how the *Drosophila* orthologs of these 40 NS genes (Table 1) modulate the function of nephrocytes (34). More than half of the NS genes listed are associated with the development of steroid-resistant nephrotic syndrome in humans, which cause ~15% of all CKD diagnosed before age 25 (1). We then used the Gal4-UAS system to direct expression of RNAi silencing transgenes in nephrocytes to

systematically knockdown *Drosophila* orthologs of the NS genes listed in Table 1 (35–37). Subsequently, we quantitatively assessed the phenotypic severity of gene knockdowns using functional assays for protein uptake and sequestration of toxic silver nitrate ( $\text{AgNO}_3$ ), adult fly survival, and average lifespan. We have also validated our system, exploring the role of mutations present in key podocytes genes (i.e. the CD2AP gene) that have been linked to the pathogenesis of NS in humans and other experimental animal model systems (38–41). More specifically, we explored the role of Cindr (the fly ortholog of CD2AP) in *Drosophila* nephrocyte function (41). We also tested the ability of human patient-derived CD2AP alleles to rescue deficiencies associated with silencing endogenous Cindr gene expression. Our findings validate the efficacy and clinical relevance of the *Drosophila* experimental model system to study pathogenic mechanisms underlying most monogenic forms of NS, and reveal the possibility of using the fly to efficiently generate patient specific (i.e. personalized) *in vivo* models of monogenic renal disease.

## Results

### Silencing of most NS gene orthologs in nephrocytes reduced hemolymph protein uptake and AgNO<sub>3</sub> sequestration

In order to assess the function of the *Drosophila* orthologous of human NS genes in nephrocytes, we employed two *in vivo* cellular assays that quantitatively assessed uptake of a fluorescent hemolymph fusion protein (ANF-RFP), and sequestration of ingested AgNO<sub>3</sub>. In the former, flies carry a transgenic construct in which a myosin heavy chain (MHC) gene promoter directs the expression of atrial natriuretic factor (ANF) (42) peptide - red fluorescent protein (RFP) fusion protein. Muscle cells expressing the MHC-ANF-RFP transgene secrete ANF-RFP fusion protein into the fly's hemolymph, from which it is normally filtered and endocytosed by nephrocytes. The resulting intracellular red fluorescence is detected by fluorescence microscopy and can be quantitated. To confirm nephrocyte cell identity, flies also carry a transgene encoding green fluorescent protein (GFP) expressed under the control of the *Drosophila Hand* gene promoter (*Hand-GFP*) (Fig. 1D-F). MHC-ANF-RFP and *Hand-GFP* transgenes are combined in flies carrying a *Dot-Gal4* driver directing nephrocyte-specific expression of a *UAS-Gene<sub>x</sub>-RNAi* transgene construct that knocks down expression of the endogenous NS gene ortholog (*i.e.* *Gene<sub>x</sub>*) target. Because off-target effects of a given RNAi silencing construct could potentially elicit a false-positive result, we tested two or more available, independent RNAi silencing lines for each gene of interest. In our over-all experience, discrepancies in induced phenotypes between lines are observed very rarely (data not shown), and such presumptive evidence of off-target effects was not encountered in this study. In the second *in vivo* functional assay, we add toxic silver nitrate (AgNO<sub>3</sub>) to the standard diet of developing larvae. Ingested AgNO<sub>3</sub> is normally taken up by nephrocytes and sequestered intracellularly, where it can be detected and the metal levels quantitated using phase contrast microscopy (Fig. 1G-I).

Table 1 lists 40 known human genes that are associated with NS. We identified *Drosophila* orthologs for all these 40 NS genes. In order to demonstrate the validity of the *Drosophila* nephrocyte model for *in vivo* investigations of mutation-associated renal disease, we conducted a systematic analysis of phenotypes induced by nephrocyte-specific RNAi based silencing of each *Drosophila* gene listed in Table 1. As shown in Figure 2, silencing of most of the genes reduced ANF-RFP fluorescence relative to wild type control nephrocytes. *Zip* and *CG32105* knockdown illustrate the variable phenotypic severity as observed in this assay, while *Ste24a* knockdown illustrates a non-significant effect. Silencing of *Mec2*, *Trpgamma*, *Zip*, *Myo61F*, and *Mys* reduced RFP below the level of detection in our assay. By contrast, RFP levels were unaffected by silencing of *Ptp10D*, *CG1674*, *Scra*, *CG10585*, *Ste24a*, and *Dally*. We observed highly similar results when we assayed AgNO<sub>3</sub> sequestration by nephrocytes in which NS gene orthologs were silenced (Fig. 3).

### Silencing of most NS gene orthologs in nephrocytes shortened adult fly life span

We observed that nephrocyte specific silencing of the majority of the NS gene orthologs shortened the average adult fly lifespan (Fig. 4A). Control wild type adult flies survived approximately 33 days on average. Significant reduction in average adult lifespan associated with nephrocyte gene silencing was observed for all genes except *Ptp10D*, *Actn*, *Form3*, *CG1674*, *Scra*, *Marcal1*, *E2f*, *Ste24a*, *Emp*, *CG32649*, and *Tsp74F*. Silencing of *Ptp10D*, *CG1674*, *Scra*, and

*Ste24a* also did not reduce protein uptake or AgNO<sub>3</sub> sequestration. Silencing of the *CG10585* gene, by contrast, reduced fly lifespan without showing the effects in our nephrocyte functional assays. This may reflect a relatively high level of sensitivity to disruption of Coenzyme Q synthesis and increased susceptibility to ROS in aging adult flies. Alternatively, reduced lifespan may in this case be due to *CG10585* knockdown in cells other than nephrocytes, as the *Dot* enhancer driving RNAi expression is also active in some neurons (43). Figure 4B shows selected survival curves that illustrate the range of phenotypes induced in gene knockdown experiments. *Mec2* gene silencing in nephrocytes was associated with 100% developmental lethality (no adult flies were produced). *Zip* knockdown was associated with nearly continuous, progressive adult mortality over the course of approximately 25 days. In the case of *CG32105* gene silencing, significant adult mortality was not observed until after day 15, followed by steady and then precipitous die-off through day 30.

### *Drosophila cindr* gene silencing rescued by normal human CD2AP gene expression but not by a patient-derived mutant CD2AP-K301M allele

The CD2AP adapter protein is critical for SD formation and maintenance, and CD2AP mutations are associated with nephrotic syndrome. CD2AP knockout mice exhibit podocyte foot process defects and die from renal failure. CD2AP associates with the NPHS1 encoded protein nephrin, the major SD filter component, and the NPHS2 gene product podocin (39,41,44).

We tested the ability of a wild type (WT) human CD2AP transgene to rescue the ANF-RFP uptake deficiency induced by silencing of the *Drosophila* ortholog *Cindr* in nephrocytes. As shown in Figure 5A and B, the CD2AP-WT transgene expression in nephrocytes can significantly rescue the functional deficit in ANF-RFP uptake in a cell background of RNAi silenced endogenous *Cindr* gene expression. We extended our analysis to test CD2AP-K301M, a renal disease patient-derived mutant CD2AP allele (41), for the rescue of *Cindr* knockdown. As shown in Figure 5A and B the mutant allele did not rescue the ANF-RFP uptake defect. Furthermore, we showed that CD2AP-WT transgene expression (in *Cindr* silenced nephrocytes) significantly increased adult fly survival, but no rescue effect was observed with CD2AP-K301M mutant allele expression (Fig. 5C-D).

### *Cindr* gene silencing led to the effacement of normal NSD and lacunar channel ultrastructure

We used transmission electron microscopy to determine if defects in uptake and accumulation of ANF-RFP and AgNO<sub>3</sub> due to *Cindr* gene silencing were associated with abnormalities in the characteristic nephrocyte NSD and lacunar channel ultrastructure (29,31). As shown in Figure 5E, in normal Control nephrocytes the lacunar channels and NSDs are regularly spaced along the circumference of the cell. A single NSD is located at the mouth of each lacunar channel. Silencing of *Cindr* expression led to loss of channels and dramatically altered NSD morphology. In place of regularly spaced, discreet pairs of opposing NSD structural units, we observed dysmorphic, flattened structures tending to fuse together into semi-continuous wavelike forms, and distinct lacunar channel ultrastructure was not evident. Expression of the CD2AP-WT transgene partially restored NSD pairing and regular spacing, while the mutant CD2AP-K301M allele failed to rescue the ultrastructural defects induced by silencing of *Cindr* (Fig. 5E).



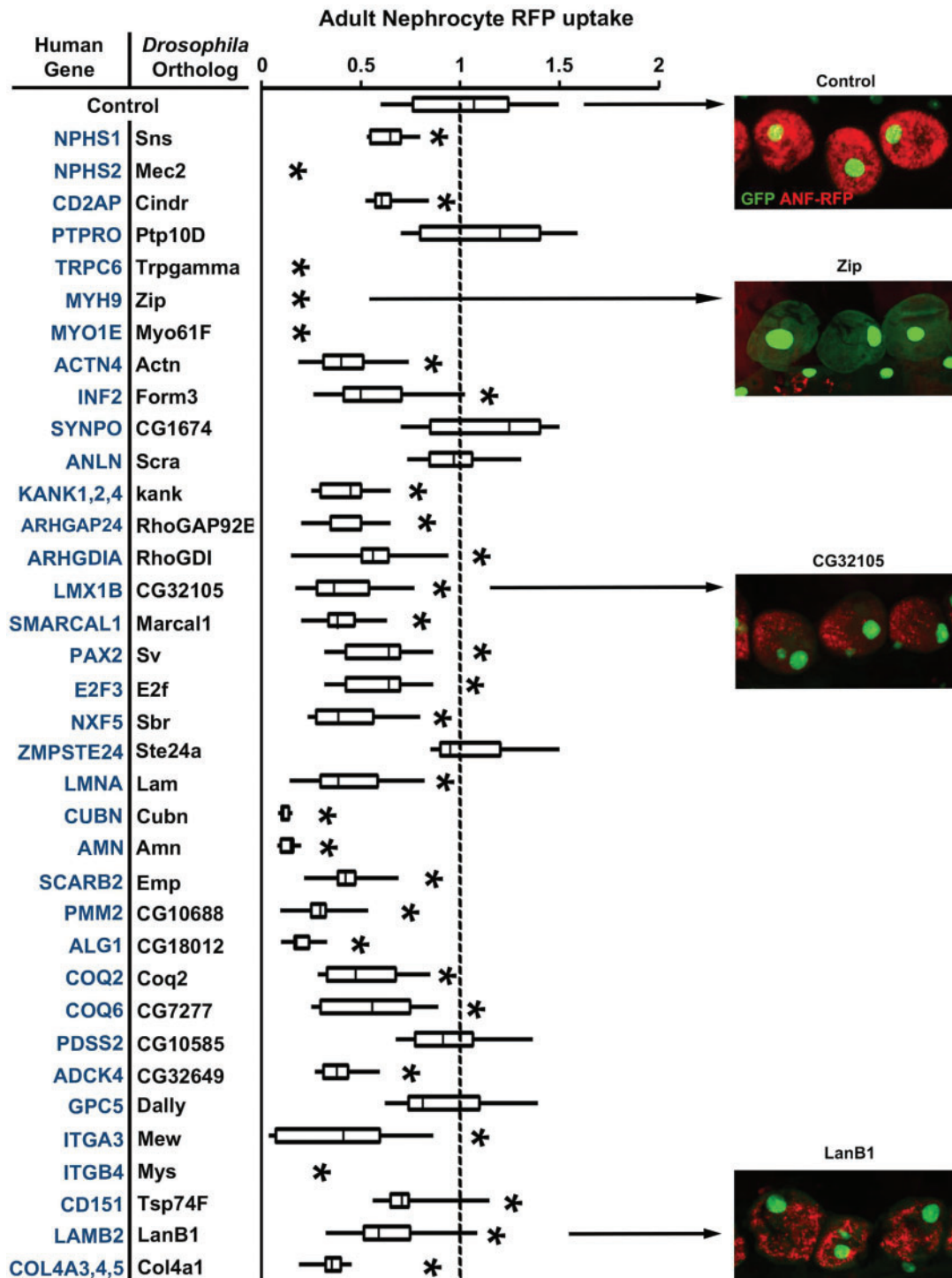


**Figure 2.** Adult Nephrocyte RFP uptake. Human NS associated genes are listed with the corresponding *Drosophila* ortholog targeted by nephrocyte expression of inhibitory RNAi transgene. RFP fluorescence in nephrocytes was assessed in transgenic flies of genotype *MHC-ANF-RFP; Hand-GFP; Dot-Gal4; UAS-Gene<sub>x</sub>-IR*. ANF-RFP fusion protein uptake levels were determined from fluorescence micrographs and expressed relative to control nephrocytes of *MHC-ANF-RFP; Hand-GFP; Dot-Gal4* transgenic flies. For quantification,  $\geq 20$  nephrocytes were analysed from each of three female flies per genotype. The results are presented as median plus interquartile range (IQR). Statistical significance (\*) was defined as  $P < 0.05$ . Example fluorescence micrographs (merged GFP and RFP fluorescence) are shown to illustrate the range of effects on RFP levels induced by RNAi silencing of different genes.

#### *Cindr* interacts with *Mec2* in *drosophila* nephrocytes

We used a genetic approach to investigate interactions between *Cindr* and other NSD proteins, informed by reported interactions between CD2AP and podocin in the podocyte SD (44).

Figure 5F and G show that nephrocytes of *Cindr<sup>+/-</sup>* and *Mec2<sup>+/-</sup>* heterozygotes are each moderately though significantly impaired in uptake of fluorescent 10 kD Dextran particles. The nephrocyte function of *Cindr<sup>+/-</sup>; Mec2<sup>+/-</sup>* double heterozygotes

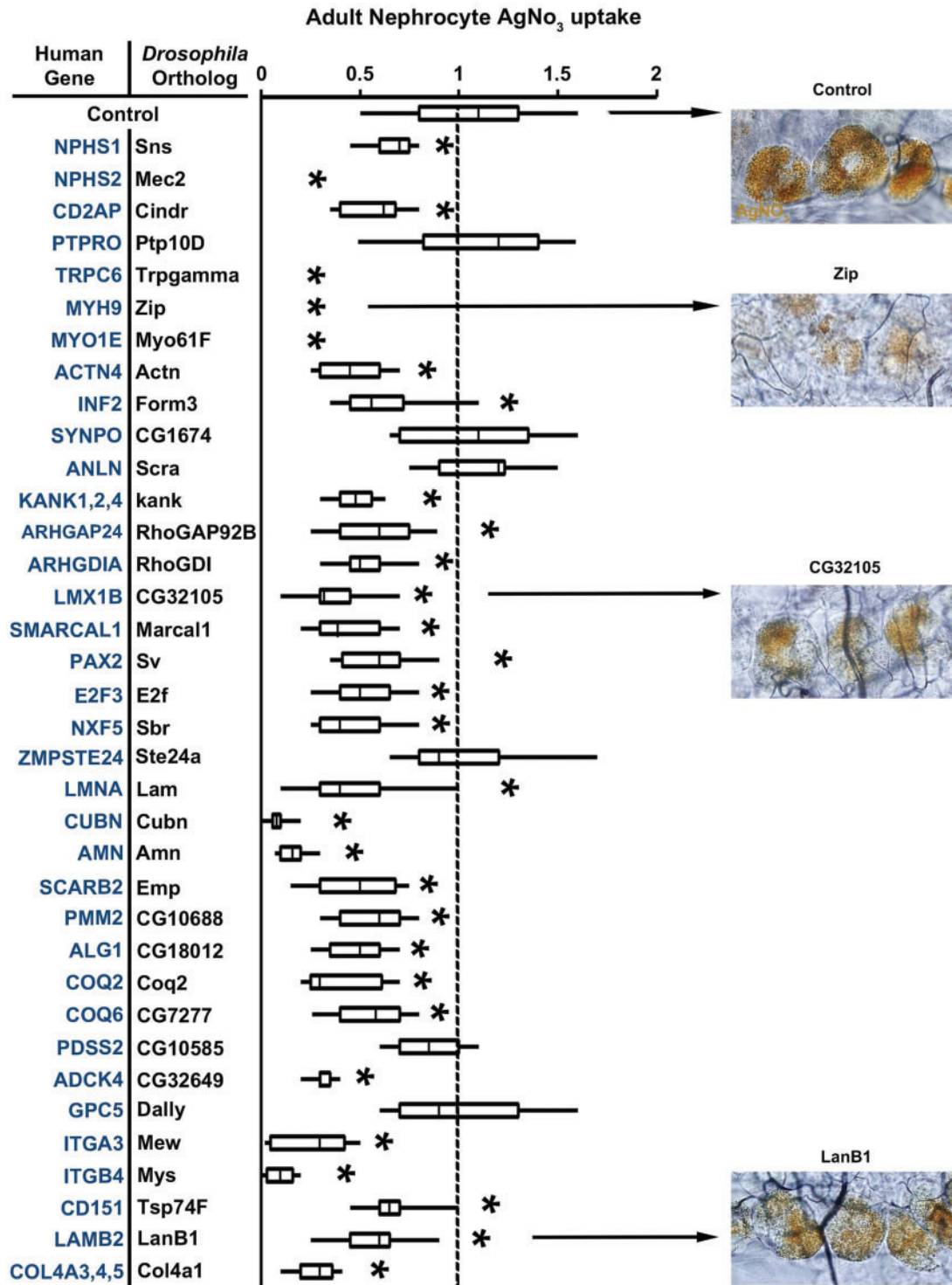
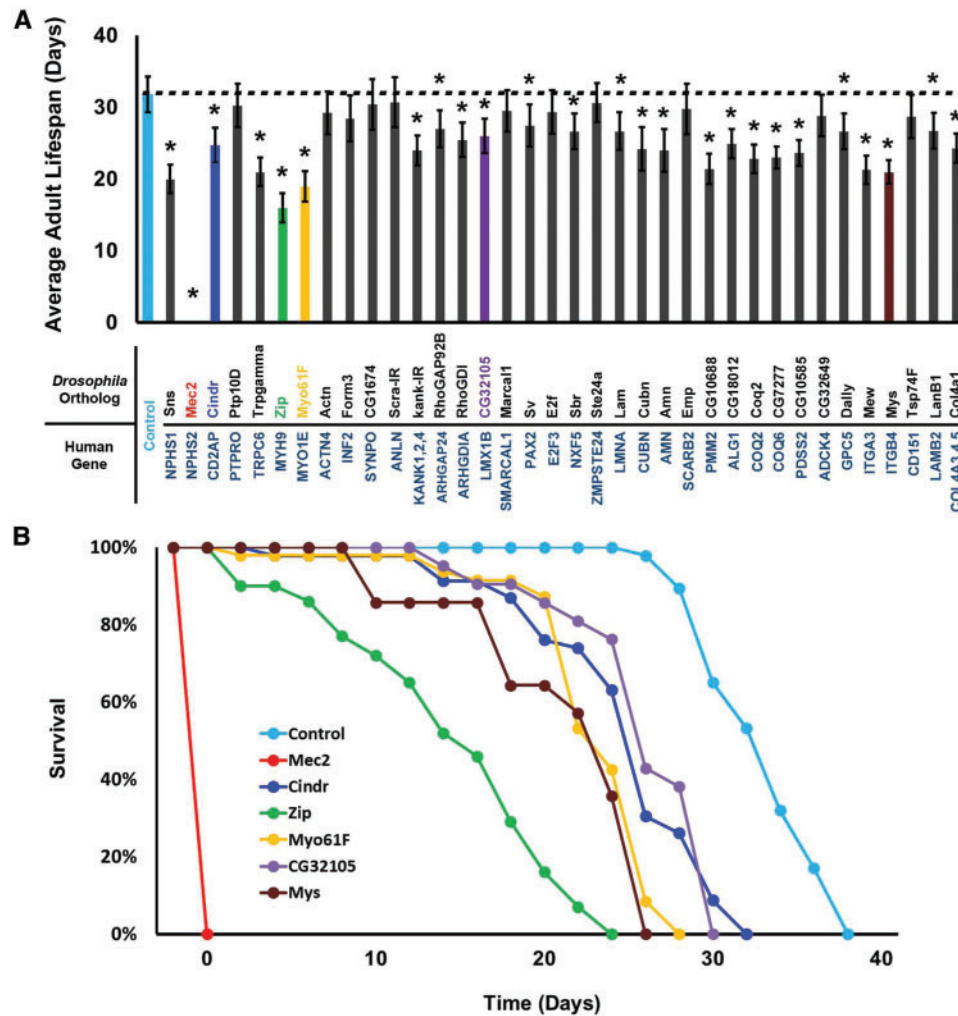


Figure 3. Adult Nephrocyte AgNO<sub>3</sub> uptake. Human NS associated genes are listed with the corresponding *Drosophila* ortholog targeted by nephrocyte expression of inhibitory RNAi transgene. AgNO<sub>3</sub> sequestration in nephrocytes was assessed in transgenic flies of genotype *Dot-Gal4; UAS-Gene<sub>x</sub>-IR*. AgNO<sub>3</sub> levels were determined from photomicrographs and expressed relative to control nephrocytes in *Dot-Gal4* transgenic flies. For quantification, ≥20 nephrocytes were analysed from each of three female flies per genotype. The results are presented as median plus interquartile range (IQR). Statistical significance (\*) was defined as *P* < 0.05. Example photomicrographs are shown to illustrate the range of effects on AgNO<sub>3</sub> levels induced by RNAi silencing of different genes.

are, in comparison to either single heterozygote, much more significantly impaired, providing *in vivo* evidence that Cindr and Mec2, like their human orthologs CD2AP and Podocin, interact and function together.

### Discussion

Rapid advances in genomic sequencing technologies have led to the identification of large numbers of potential disease genes.



**Figure 4.** Nephrocyte specific gene silencing effects on adult fly survival. (A) Effect of gene silencing on average adult life span. NS associated genes are listed with the corresponding *Drosophila* ortholog targeted by nephrocyte expression of inhibitory RNAi transgene. Lifespan was assessed in transgenic flies of genotype *Dot-Gal4; UAS-Gene<sub>x</sub>-IR* and Control flies of genotype *Dot-Gal4*. 50 flies of each genotype were maintained at 29 °C (to increase Gal4 driven RNAi transgene expression) and mortality was recorded every 48 hours until all flies were dead. Experiments were performed in triplicate. The results are presented as average life span (in days). The results are presented as SEM. Statistical significance (\*) was defined as  $P < 0.05$ . Colored histograms correspond to example survival curves shown in B. (B) Example survival curves for flies expressing the indicated gene silencing constructs. The curves correspond to the colored histograms in (A). *Mec2* gene silencing was developmentally lethal, with no adult emergence from the pupa stage.

To fully capitalize on these advances, a high-throughput animal model is required to provide disease-relevant functional data. As described here, we have established the *Drosophila* nephrocyte system as such a high-throughput functional validation system for nephrotic syndrome, an important type of renal disease. As proof-of-principle, we showed that 34 out of 40 known NS gene orthologs are required for nephrocyte function, using quantitative assays for protein uptake and sequestration of toxic  $\text{AgNO}_3$ . Based on our observations approximately 85% of the identified NS genes have conserved roles in renal function from flies to humans, showing that *Drosophila* is a valuable simple animal model in which to investigate a majority of NS genes.

Of the 40 NS genes addressed in this study, 33 had previously been analysed for effects on kidney cell biology in mouse and/or zebrafish models. To our knowledge, the current study is the first published report of renal cell phenotypes induced by knockdown of *NXF5*, *LMNA*, *PMM2*, *ALG1*, *COQ2*, and *ITGB4* gene homologs in an animal model system (*ZMPSTE24* knockdown

has also not previously been described in the context of model kidney studies, but we were unable to detect an *Ste24a* RNAi silencing induced phenotype in our assays). *NXF5* mutations are associated with FSGS (42). Knockout of the mouse functional ortholog, *Nxf7*, was shown to impair memory but effects on kidney function were not examined (45). In mice, knockdown of *Zmpste24* and *Lmna* caused a rapid aging phenotype (46) and deletion of *Lmna* led to growth delay and reduced body weight (47). Renal deficiencies, however, were not reported. Thus, a comprehensive functional analysis employing *Drosophila* nephrocytes has yielded novel observations on the physiological consequences of known NS gene silencing *in vivo*.

Furthermore, for 25 of the tested *Drosophila* genes, silencing in nephrocytes was associated with reduced adult fly lifespan, indicating that the compromised nephrocyte function was frequently associated with increased mortality. Effects on lifespan may be due to reduced nephrocyte function leading to deficiencies in reabsorption of proteins and recycling of metabolic resources and/or failure to sequester harmful metabolic waste products which eventually



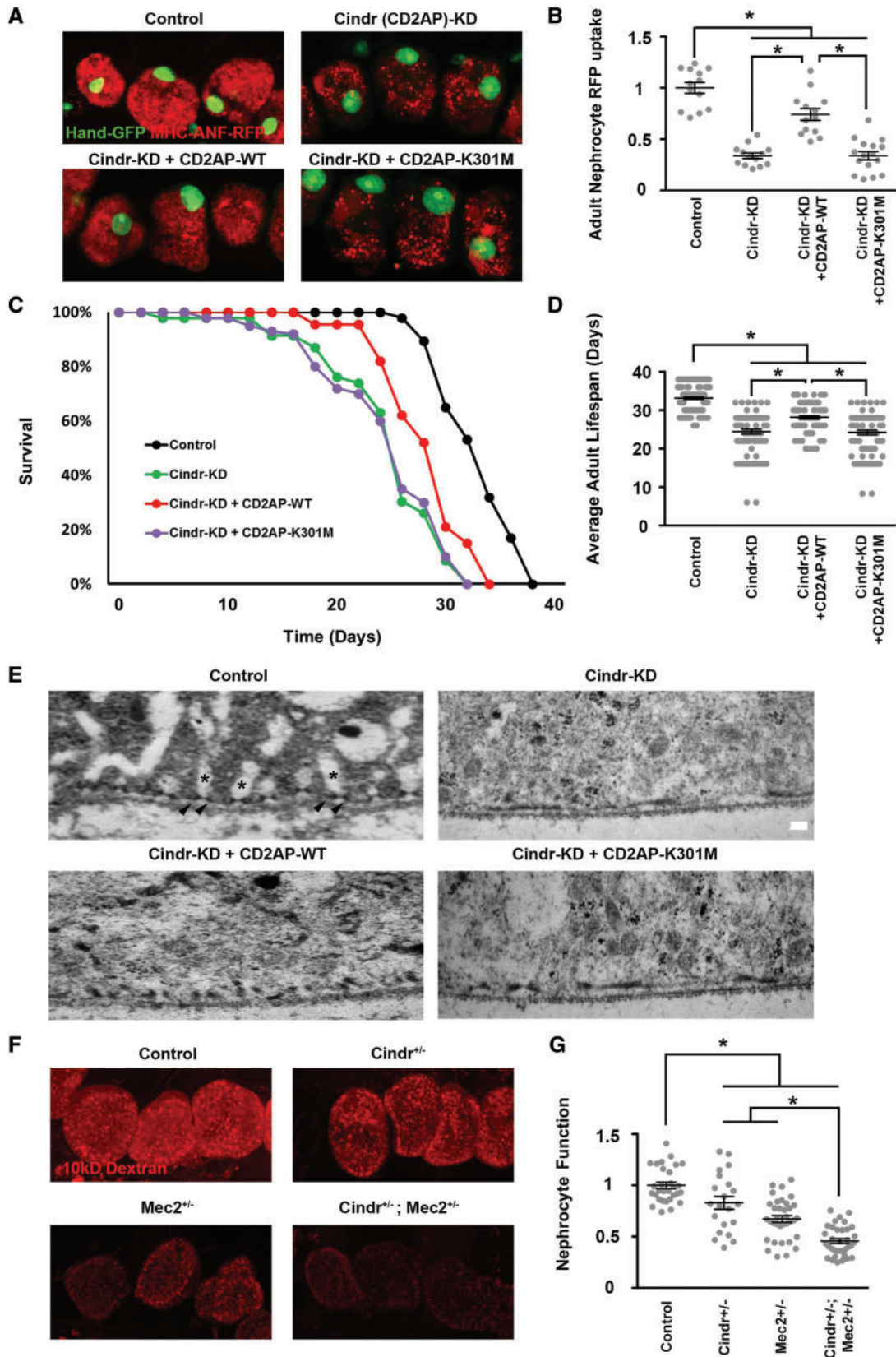


Figure 5. *Cindr* is required for nephrocyte function, fly survival, and nephrocyte cell ultrastructure; *Cindr* gene silencing can be rescued by a normal but not a patient-derived mutant allele of human CD2AP; *Cindr* interacts with *Mec2* in nephrocytes. (A). ANF-RFP uptake visualized by fluorescence microscopy in nephrocytes of Control flies (genotype *Hand-GFP; Dot-Gal4*), *Cindr* (CD2AP)-KD flies in which *Cindr* expression was silenced in nephrocytes with a *Cindr* targeting RNAi construct (genotype



compromise fly health. Alternatively, nephrocyte physiological dysfunction may eventually render the nephrocyte itself harmful to the fly, for example through accumulation of ROS or other intermediaries of cellular stress. In either case, our observations suggest that *Drosophila* can indeed model pathogenic features of life threatening renal disease. Disparities between the severity of RFP and AgNO<sub>3</sub> functional phenotypes and less severe effects on longevity may be explained by the optimal environmental conditions in which these flies were maintained, which are known to preserve their renal function. To test this hypothesis, we are currently testing the effects of gene silencing on adult survival for flies maintained under stress from toxin exposure.

In order to further confirm the function of a particular renal gene and exploit the nephrocyte model as a powerful *in vivo* experimental platform to explore the pathogenesis of NS in humans, we focused our attention on *Cindr*, the *Drosophila* ortholog of CD2AP, a well-studied monogenic risk factor for NS (39,41,48). We found that the diminished nephrocyte protein uptake induced by silencing *Cindr* was rescued by expression of a normal allele of human CD2AP, but not by a patient derived mutant allele. Differential rescue capabilities were also observed for adult fly lifespan, and nephrocyte cell ultrastructural features dependent upon CD2AP protein function. CD2AP has been reported to function as a linker protein associated with the podocyte SD where it has been shown to interact with both nephrin and podocin (44,48). We used genetics to show that in nephrocytes, *Cindr* interacts with *Mec2*, the *Drosophila* gene encoding the podocin homolog. This result confirms the similarities in organization of SD/NSD components at the molecular level in nephrocytes and podocytes, and extends earlier studies conducted in garland nephrocytes during *Drosophila* embryonic development (31).

Interestingly, six of the NS gene fly homologs tested by silencing in nephrocytes (*Ptp10D*, *CG1674*, *Scra*, *Ste24a*, *CG10585*, and *Dally*) did not induce functional deficiencies in our assays. In the case of *Dally* (the *GPC5* homolog), this result was consistent with previous studies showing that *GPC5* risk is associated with higher expression, and that podocyte-specific knockdown of gene expression actually confers resistance to cellular injury (49). *Ste24a* encodes a metalloprotease involved in the generation of mature lamin A, and mutations in the human homolog *ZMPSTE24* are associated with FSGS (50). It has been reported that disease severity is correlated with levels of residual *ZMPSTE24* enzyme activity, with complete loss-of-function alleles associated with the most severe disease manifestations (51). It is not unreasonable, therefore, to suggest that the degree

of silencing of *Ste24a* by RNAi in nephrocytes may have been below the level required for detection in our assays. That lamin A production is important in nephrocytes as it is in podocytes, however, was clearly shown by the functional deficits induced by silencing of the *LMNA* homolog *lam*.

The complex cytoarchitecture of the podocyte and the cell's ability to withstand the forces associated with blood filtration are critically supported by the actin cytoskeleton (52). Podocyte injury leads to cytoskeletal disruptions that commonly result in foot process effacement and proteinuria (53,54). Although the *Drosophila* nephrocyte is not subjected to the rigorous physical challenges associated with blood filtration under high pressure, we found that seven of nine homologs of NS genes associated with actin cytoskeletal dynamics displayed knock down phenotypes in our functional assays. *RhoGDI* and *Kank* gene silencing had previously been shown to impair nephrocyte function and disrupt NSD and the lacunar channel structure (12,26). These observations underscore the functional, structural, and regulatory linkages between slit diaphragm filtration and the actin cytoskeleton. The *Drosophila* nephrocyte model system can be a highly useful experimental platform to dissect *in vivo* and at high resolution the molecular interactions underlying these linkages.

Mutations in the genes *COQ2*, *COQ6*, *PDSS2*, and *ADCK4* encoding enzymes involved in the biosynthesis of Coenzyme Q10 (CoQ10) are associated with NS (14,15,55,56). CoQ10 plays an essential role in the mitochondrial respiratory chain and protects against damage from reactive oxygen species (ROS) (56–58). Our observations indicate that nephrocyte functions are also susceptible to CoQ10 deficiency induced by knockdown of biosynthetic enzyme activity. Additional ongoing studies indicate that these phenotypes are associated with elevated ROS and cytotoxicity (data not shown).

It has recently been reported that collagen IV mutations are frequently associated with FSGS and SRNS (59). We observed that nephrocyte specific silencing of *Drosophila* *Col4A1* induced functional defects and shortened fly average lifespan. The critical importance of extracellular matrix and actin cytoskeleton in both nephrocyte and podocyte function was further emphasized by our finding that silencing of the *Drosophila* integrin genes *Mew* and *Mys* (homologs of human *ITGA3* and *ITGB4*, respectively) led to severe functional defects and lifespan reduction. Integrins are known to be essential in podocytes, and integrin gene mutations are associated with nephrotic syndrome (60).

A number of genes associated with NS play roles in the nucleus, including transcription and RNA export. We observed

---

*Hand-GFP*; *Dot-Gal4*; *UAS-Cindr-RNAi*), *Cindr-KD* + *CD2AP-WT* flies in which a transgenic wild type allele of human CD2AP was expressed simultaneously with *Cindr* -targeting RNAi (genotype *Hand-GFP*; *Dot-Gal4*; *UAS-Cindr-RNAi*; *UAS-CD2AP*), and *Cindr-KD* + *CD2AP-K301M* flies in which a transgenic mutant allele of human CD2AP was expressed simultaneously with *Cindr* -targeting RNAi (genotype *Hand-GFP*; *Dot-Gal4*; *UAS-Cindr-RNAi*; *UAS-CD2AP-K301M*). The panels show merged ANF-RFP (54) and GFP (green, mostly nuclear) fluorescence. (B) Quantification of nephrocyte RFP levels relative to Control flies. For quantification,  $\geq 20$  nephrocytes were analysed from each of three female flies per genotype. The results are presented as mean  $\pm$  s.e.m. Statistical significance (\*) was defined as  $P < 0.05$ . (C) Adult fly survival curves illustrating effects on longevity of *Cindr* silencing and extent of rescue from expression of WT and mutant alleles of human CD2AP. 50 flies of each genotype were maintained at 29°C (to increase Gal4 driven RNAi transgene expression) and mortality was recorded every 48 hours until all flies were dead. Triplicate samples were analysed. (D) Average adult lifespan showing effects of *Cindr* silencing and rescue by WT and mutant alleles of human CD2AP. 50 flies of each genotype were maintained at 29°C (to increase Gal4 driven RNAi transgene expression) and mortality was recorded every 48 hours until all flies were dead. Experiments were performed in triplicate. The results are presented as mean  $\pm$  s.e.m. Statistical significance (\*) was defined as  $P < 0.05$ . (E) Transmission electron microscopy showing effects on nephrocyte NSD (arrowheads) and lacunar channel (\*) ultrastructure of *Cindr* gene silencing and the extent of rescue from expression of WT and mutant alleles of human CD2AP. In Control nephrocytes NSDs were regularly and precisely spaced along the entire circumference of the cell and spanned the "mouth" of each lacunar channel. Silencing *Cindr* gene expression led to fusion of NSDs and the loss of lacunar channels. Expression of WT human CD2AP significantly rescued the ultrastructural defects, while the mutant CD2AP allele had very little effect. (F) Functional interaction between *Cindr* and *Mec2* in nephrocytes demonstrated by *Cindr*<sup>+/-</sup>; *Mec2*<sup>+/-</sup> double heterozygote synergistic enhancement of deleterious effect on uptake of fluorescent Dextran particles in comparison to *Cindr*<sup>+/-</sup> or *Mec2*<sup>+/-</sup> single heterozygotes. (G). Quantitative analysis of fluorescent Dextran levels in nephrocytes of the indicated genotype, expressed relative to Control. For quantification,  $\geq 20$  nephrocytes were analysed from each of three female flies per genotype. The results are presented as mean  $\pm$  s.e.m. Statistical significance (\*) was defined as  $P < 0.05$ .

that *Drosophila* homologs of these genes are essential for nephrocyte function. For example, the homeobox transcription factor *LMX1B* is involved in the maintenance of the actin cytoskeleton and regulation of the SD, and *LMX1B* haploinsufficiency is associated with NS (61,62). We observed strong functional phenotypes and reduced fly lifespan induced by nephrocyte specific silencing of the *Drosophila* homolog *CG32105*.

Overall, our findings show that of human genes known to be associated with NS, a majority of them play conserved roles in renal function from flies to humans. We conclude that the *Drosophila* nephrocyte can be used both to elucidate clinically relevant molecular mechanisms underlying the pathogenesis of most monogenic forms of NS, and efficiently generate patient-specific *in vivo* models of genetic renal diseases caused by specific mutations.

## Materials and Methods

### Fly strains

Flies were reared on standard fly food at room temperature, or at 29°C for experiments involving Gal4 (to boost the activity of the yeast-derived Gal4 protein). Flies carrying *Hand-GFP*, *Dot-Gal4*, *MHC-ANF-RFP* transgenes were described previously (30,63). All RNAi based gene silencing lines were obtained from the Bloomington *Drosophila* Stock Center except for the *Sns* targeting line, which was from the Vienna *Drosophila* Resource Center. Flies with multiple transgenes were generated using standard genetic methods.

### DNA cloning and generation of transgenic fly strains

A normal human CD2AP cDNA was obtained from OriGene, which encodes the common 639 a.a. isoform with NCBI reference sequence NP\_036252. The cDNA of CD2AP-K301M mutation identified from a NS patient (41) was generated using QuikChange Site-Directed Mutagenesis Kit (Clontech) from a wild-type CD2AP cDNA. This wild-type and mutant CD2AP cDNA are only different at the lysine 301. To generate UAS-CD2AP and UAS-CD2AP-K301M constructs, the above cDNAs were cloned into the pUAST vector and introduced into the germ cells of flies by standard P element-mediated germ line transformation.

### RFP uptake assay

Flies of the appropriate genotypes were allowed to lay eggs at 25°C. One day after egg laying, embryos were shifted to 29°C. RFP uptake by pericardial nephrocytes was assessed in adult flies one day post-emergence by dissecting heart tissues into *Drosophila* Schneider's Medium (ThermoFisher) and examining the cells by fluorescence microscopy. For quantification,  $\geq 20$  nephrocytes were analysed from each of three flies per genotype.

### AgNO<sub>3</sub> uptake assay

Flies of the appropriate genotype were allowed to lay eggs on standard apple juice plates for 24 hours. Freshly emerged first instar larvae were transferred to agar-only plates supplemented with a regular yeast paste containing AgNO<sub>3</sub> (2.0 g yeast in 3.5 ml 0.0005% AgNO<sub>3</sub> solution) and allowed to develop at 29°C until adulthood. AgNO<sub>3</sub> uptake by pericardial nephrocytes was assessed in adult flies one day post-emergence by

dissecting heart tissues into *Drosophila* Schneider's Medium (ThermoFisher) and examining the cells by phase contrast microscopy. For quantification,  $\geq 20$  nephrocytes were analysed from each of three female flies per genotype.

### Survival assay

Flies of the appropriate genotype were allowed to lay eggs at 25°C. One day after egg collection, embryos were shifted to 29°C and animals were maintained at that temperature throughout subsequent development and adulthood. Within one day of emergence, a total of 50 adult male flies of a given genotype were transferred to fresh vials at  $\leq 15$  per vial. Triplicate samples were analysed. Vials were checked and mortality recorded every 48 hours until all flies were dead.

### Dextran uptake assay

Flies of the appropriate genotypes were allowed to lay eggs at 25°C. One day after egg laying embryos were shifted to 29°C. Dextran uptake by pericardial nephrocytes was assessed *ex vivo* in adult flies one-day post-emergence by dissecting heart tissues into *Drosophila* Schneider's Medium (Thermo Fisher) and examining the cells by fluorescence microscopy after 20 min incubation with AlexaFluo568-Dextran (10 kD, 0.05 mg/ml). For quantification,  $\geq 20$  nephrocytes were analysed from each of three flies per genotype.

### Light microscopy and confocal imaging

*Drosophila* tissues were dissected and fixed for 10 minutes in 4% paraformaldehyde in phosphate-buffered saline (PBS). Confocal imaging was performed with a Zeiss ApoTome.2 microscope using a 20× Plan-Apochromat 0.8 N.A. air objective. For quantitative image comparisons common settings were chosen to avoid oversaturation. ImageJ Software Version 1.49 was used for image processing.

### Statistical analysis

Statistical tests were performed using PAST.exe software (<http://folk.uio.no/ohammer/past/index.html>) unless otherwise noted. Sample errors are given as standard error of the mean (s.e.m). Data were first tested for normality by using the Shapiro-Wilk test ( $\alpha = 0.05$ ). Normally distributed data were analysed either by Student's t-test (two groups) and Bonferroni comparison to adjust the P value or by a one-way analysis of variance followed by a Tukey-Kramer post-test for comparing multiple groups. Non-normal distributed data were analysed by either a Mann-Whitney test (two groups) and Bonferroni comparison to adjust P value or a Kruskal-Wallis H-test followed by a Dunn's test for comparisons between multiple groups. Statistical significance was defined as  $P < 0.05$ .

### TEM

TEM was carried out using established, standard procedures (29). Briefly, flies of the indicated genotype were fixed with Sorensen phosphate buffer containing 4% paraformaldehyde and 2.5% glutaraldehyde. The processed samples were analysed using a Philips CM100 TEM.

## Acknowledgements

We thank the Bloomington Stock Center and the Vienna Drosophila Resource Center for providing fly stocks.

Conflict of Interest statement. None declared.

## Funding

Z.H. is supported by the National Institute of Health (NIH) R01 grant DK098410. P.E.R. is supported by NIH R01 grants DK49419, DK103564, DK108368.

## References

- Sadowski, C.E., Lovric, S., Ashraf, S., Pabst, W.L., Gee, H.Y., Kohl, S., Engelmann, S., Vega-Warner, V., Fang, H., Halbritter, J., et al. (2015) A single-gene cause in 29.5% of cases of steroid-resistant nephrotic syndrome. *J. Am. Soc. Nephrol.*, **26**, 1279–1289.
- Hildebrandt, F. (2010) Genetic kidney diseases. *Lancet*, **375**, 1287–1295.
- Vivante, A., Kohl, S., Hwang, D.Y., Dworschak, G.C. and Hildebrandt, F. (2014) Single-gene causes of congenital anomalies of the kidney and urinary tract (CAKUT) in humans. *Pediatr. Nephrol.*, **29**, 695–704.
- Devuyst, O., Knoers, N.V., Remuzzi, G. and Schaefer, F. and Board of the Working Group for Inherited Kidney Diseases of the European Renal Association and European Dialysis and Transplant Association (2014) Rare inherited kidney diseases: challenges, opportunities, and perspectives. *Lancet*, **383**, 1844–1859.
- Vivante, A. and Hildebrandt, F. (2016) Exploring the genetic basis of early-onset chronic kidney disease. *Nat. Rev. Nephrol.*, **12**, 133–146.
- Smoyer, W.E. and Mundel, P. (1998) Regulation of podocyte structure during the development of nephrotic syndrome. *J. Mol. Med.*, **76**, 172–183.
- Lovric, S., Ashraf, S., Tan, W. and Hildebrandt, F. (2015) Genetic testing in steroid-resistant nephrotic syndrome: when and how?. *Nephrol. Dial. Transplant*, **31**, 1802–1813.
- Greka, A. and Mundel, P. (2012) Cell biology and pathology of podocytes. *Ann. Rev. Physiol.*, **74**, 299–323.
- Greka, A. (2016) Human genetics of nephrotic syndrome and the quest for precision medicine. *Curr. Opin. Nephrol. Hypertens*, **25**, 138–143.
- Boute, N., Gribouval, O., Roselli, S., Benessy, F., Lee, H., Fuchshuber, A., Dahan, K., Gubler, M.C., Niaudet, P. and Antignac, C. (2000) NPHS2, encoding the glomerular protein podocin, is mutated in autosomal recessive steroid-resistant nephrotic syndrome. *Nat. Gen.*, **24**, 349–354.
- Kestila, M., Lenkkeri, U., Mannikko, M., Lamerdin, J., McCready, P., Putaala, H., Ruotsalainen, V., Morita, T., Nissinen, M., Herva, R., et al. (1998) Positionally cloned gene for a novel glomerular protein–nephrin—is mutated in congenital nephrotic syndrome. *Mol. Cell*, **1**, 575–582.
- Gee, H.Y., Saisawat, P., Ashraf, S., Hurd, T.W., Vega-Warner, V., Fang, H., Beck, B.B., Gribouval, O., Zhou, W., Diaz, K.A., et al. (2013) ARHGDI mutations cause nephrotic syndrome via defective RHO GTPase signaling. *J. Clin. Invest.*, **123**, 3243–3253.
- Kambham, N., Tanji, N., Seigle, R.L., Markowitz, G.S., Pulkkinen, L., Uitto, J. and D'Agati, V.D. (2000) Congenital focal segmental glomerulosclerosis associated with beta4 integrin mutation and epidermolysis bullosa. *Am. J. Kidney Dis.*, **36**, 190–196.
- Ashraf, S., Gee, H.Y., Woerner, S., Xie, L.X., Vega-Warner, V., Lovric, S., Fang, H., Song, X., Cattran, D.C., Avila-Casado, C., et al. (2013) ADCK4 mutations promote steroid-resistant nephrotic syndrome through CoQ10 biosynthesis disruption. *J. Clin. Invest.*, **123**, 5179–5189.
- Heeringa, S.F., Chernin, G., Chaki, M., Zhou, W., Sloan, A.J., Ji, Z., Xie, L.X., Salviati, L., Hurd, T.W. and Vega-Warner, V. (2011) COQ6 mutations in human patients produce nephrotic syndrome with sensorineural deafness. *J. Clin. Invest.*, **121**, 2013–2024.
- Ovunc, B., Otto, E.A., Vega-Warner, V., Saisawat, P., Ashraf, S., Ramaswami, G., Fathy, H.M., Schoeb, D., Chernin, G., Lyons, R.H., et al. (2011) Exome sequencing reveals cubilin mutation as a single-gene cause of proteinuria. *J. Am. Soc. Nephrol.*, **22**, 1815–1820.
- Montgomery, E., Sayer, J.A., Baines, L.A., Hynes, A.M., Vega-Warner, V., Johnson, S., Goodship, J.A. and Otto, E.A. (2015) Novel compound heterozygous mutations in AMN cause Imerslund-Grasbeck syndrome in two half-sisters: a case report. *BMC Med. Genet.*, **16**, 35.
- Inoue, K. and Ishibe, S. (2015) Podocyte endocytosis in the regulation of the glomerular filtration barrier. *Am. J. Physiol. Renal Physiol.*, **309**, F398–F405.
- Winn, M.P., Conlon, P.J., Lynn, K.L., Farrington, M.K., Creazzo, T., Hawkins, A.F., Daskalakis, N., Kwan, S.Y., Ebersviller, S., Burchette, J.L., et al. (2005) A mutation in the TRPC6 cation channel causes familial focal segmental glomerulosclerosis. *Science*, **308**, 1801–1804.
- He, B., Ebarasi, L., Zhao, Z., Guo, J., Ojala, J.R., Hultenby, K., De Val, S., Betsholtz, C. and Tryggvason, K. (2014) Lmx1b and FoxC combinatorially regulate podocin expression in podocytes. *J. Am. Soc. Nephrol.*, **25**, 2764–2777.
- Bier, E. (2005) Drosophila, the golden bug, emerges as a tool for human genetics. *Nat. Rev. Genet.*, **6**, 9–23.
- Denholm, B. and Skaer, H. (2009) Bringing together components of the fly renal system. *Curr. Opin. Genet. Dev.*, **19**, 526–532.
- Dow, J.A. and Romero, M.F. (2010) Drosophila provides rapid modeling of renal development, function, and disease. *Am. J. Physiol. Renal Physiol.*, **299**, F1237–F1244.
- Simons, M. and Huber, T.B. (2009) Flying podocytes. *Kidney Int.*, **75**, 455–457.
- Na, J. and Cagan, R. (2013) The Drosophila nephrocyte: back on stage. *J. Am. Soc. Nephrol.*, **24**, 161–163.
- Gee, H.Y., Zhang, F., Ashraf, S., Kohl, S., Sadowski, C.E., Vega-Warner, V., Zhou, W., Lovric, S., Fang, H., Nettleton, M., et al. (2015) KANK deficiency leads to podocyte dysfunction and nephrotic syndrome. *J. Clin. Invest.*, **125**, 2375–2384.
- Reiter, L.T., Potocki, L., Chien, S., Gribskov, M. and Bier, E. (2001) A systematic analysis of human disease-associated gene sequences in Drosophila melanogaster. *Genome Res.*, **11**, 1114–1125.
- Chien, S., Reiter, L.T., Bier, E. and Gribskov, M. (2002) Homophila: human disease gene cognates in Drosophila. *Nucleic Acids Res.*, **30**, 149–151.
- Zhang, F., Zhao, Y., Chao, Y., Muir, K. and Han, Z. (2013) Cubilin and amnionless mediate protein reabsorption in Drosophila nephrocytes. *J. Am. Soc. Nephrol.*, **24**, 209–216.
- Zhang, F., Zhao, Y. and Han, Z. (2013) An in vivo functional analysis system for renal gene discovery in Drosophila pericardial nephrocytes. *J. Am. Soc. Nephrol.*, **24**, 191–197.



31. Weavers, H., Prieto-Sanchez, S., Grawe, F., Garcia-Lopez, A., Artero, R., Wilsch-Brauninger, M., Ruiz-Gomez, M., Skaer, H. and Denholm, B. (2009) The insect nephrocyte is a podocyte-like cell with a filtration slit diaphragm. *Nature*, **457**, 322–326.
32. Zhuang, S., Shao, H., Guo, F., Trimble, R., Pearce, E. and Abmayr, S. (2009) Sns and Kirre, the Drosophila orthologs of Neph1 and Neph3, direct adhesion, fusion and formation of a slit diaphragm-like structure in insect nephrocytes. *Development*, **136**, 2335–2344.
33. Hu, Y., Flockhart, I., Vinayagam, A., Bergwitz, C., Berger, B., Perrimon, N. and Mohr, S.E. (2011) An integrative approach to ortholog prediction for disease-focused and other functional studies. *BMC Bioinformatics*, **12**, 357.
34. Bierzyska, A., Soderquest, K. and Koziell, A. (2014) Genes and podocytes - new insights into mechanisms of podocytopathy. *Front. Endocrinol.*, **5**, 226.
35. Ni, J.Q., Markstein, M., Binari, R., Pfeiffer, B., Liu, L.P., Villalta, C., Booker, M., Perkins, L. and Perrimon, N. (2008) Vector and parameters for targeted transgenic RNA interference in *Drosophila melanogaster*. *Nat. Methods*, **5**, 49–51.
36. Ni, J.Q., Zhou, R., Czech, B., Liu, L.P., Holderbaum, L., Yang-Zhou, D., Shim, H.S., Tao, R., Handler, D. and Karpowicz, P. (2011) A genome-scale shRNA resource for transgenic RNAi in *Drosophila*. *Nat. Methods*, **8**, 405–407.
37. Brand, A.H. and Perrimon, N. (1993) Targeted gene expression as a means of altering cell fates and generating dominant phenotypes. *Development*, **118**, 401–415.
38. Kim, J.M., Wu, H., Green, G., Winkler, C.A., Kopp, J.B., Miner, J.H., Unanue, E.R. and Shaw, A.S. (2003) CD2-associated protein haploinsufficiency is linked to glomerular disease susceptibility. *Science*, **300**, 1298–1300.
39. Shih, N.Y., Li, J., Karpitskii, V., Nguyen, A., Dustin, M.L., Kanagawa, O., Miner, J.H. and Shaw, A.S. (1999) Congenital nephrotic syndrome in mice lacking CD2-associated protein. *Science*, **286**, 312–315.
40. Lowik, M., Levtchenko, E., Westra, D., Groenen, P., Steenbergen, E., Weening, J., Lilien, M., Monnens, L. and van den Heuvel, L. (2008) Bigenic heterozygosity and the development of steroid-resistant focal segmental glomerulosclerosis. *Nephrol. Dial. Transplant*, **23**, 3146–3151.
41. Gigante, M., Pontrelli, P., Montemurro, E., Roca, L., Aucella, F., Penza, R., Caridi, G., Ranieri, E., Ghiggeri, G.M. and Gesualdo, L. (2009) CD2AP mutations are associated with sporadic nephrotic syndrome and focal segmental glomerulosclerosis (FSGS). *Nephrol. Dial. Transplant*, **24**, 1858–1864.
42. Esposito, T., Lea, R.A., Maher, B.H., Moses, D., Cox, H.C., Magliocca, S., Angius, A., Nyholt, D.R., Titus, T., Kay, T., et al. (2013) Unique X-linked familial FSGS with co-segregating heart block disorder is associated with a mutation in the NXF5 gene. *Hum. Mol. Genet.*, **22**, 3654–3666.
43. Krupp, J.J., Billeter, J.C., Wong, A., Choi, C., Nitabach, M.N. and Levine, J.D. (2013) Pigment-dispersing factor modulates pheromone production in clock cells that influence mating in *Drosophila*. *Neuron*, **79**, 54–68.
44. Schwarz, K., Simons, M., Reiser, J., Saleem, M.A., Faul, C., Kriz, W., Shaw, A.S., Holzman, L.B. and Mundel, P. (2001) Podocin, a raft-associated component of the glomerular slit diaphragm, interacts with CD2AP and nephrin. *J. Clin. Invest.*, **108**, 1621–1629.
45. Vanmarsenille, L., Verbeeck, J., Belet, S., Roebroek, A.J., Van de Putte, T., Nevelsteen, J., Callaerts-Vegh, Z., D'Hooge, R., Marynen, P. and Froyen, G. (2013) Generation and characterization of an *Nxf7* knockout mouse to study NXF5 deficiency in a patient with intellectual disability. *PLoS One*, **8**, e64144.
46. Varela, I., Cadinanos, J., Pendas, A.M., Gutierrez-Fernandez, A., Folgueras, A.R., Sanchez, L.M., Zhou, Z., Rodriguez, F.J., Stewart, C.L., Vega, J.A., et al. (2005) Accelerated ageing in mice deficient in *Zmpste24* protease is linked to p53 signaling activation. *Nature*, **437**, 564–568.
47. Ruan, J., Liu, X.G., Zheng, H.L., Li, J.B., Xiong, X.D., Zhang, C.L., Luo, C.Y., Zhou, Z.J., Shi, Q. and Weng, Y.G. (2014) Deletion of the *lmna* gene induces growth delay and serum biochemical changes in C57BL/6 mice. *Asian-Australas. J. Anim. Sci.*, **27**, 123–130.
48. Shih, N.Y., Li, J., Cotran, R., Mundel, P., Miner, J.H. and Shaw, A.S. (2001) CD2AP localizes to the slit diaphragm and binds to nephrin via a novel C-terminal domain. *Am. J. Pathol.*, **159**, 2303–2308.
49. Okamoto, K., Tokunaga, K., Doi, K., Fujita, T., Suzuki, H., Katoh, T., Watanabe, T., Nishida, N., Mabuchi, A. and Takahashi, A. (2011) Common variation in *GPC5* is associated with acquired nephrotic syndrome. *Nat. Genet.*, **43**, 459–463.
50. Agarwal, A.K., Zhou, X.J., Hall, R.K., Nicholls, K., Bankier, A., Van Esch, H., Fryns, J.P. and Garg, A. (2006) Focal segmental glomerulosclerosis in patients with mandibuloacral dysplasia owing to ZMPSTE24 deficiency. *J. Invest. Med.*, **54**, 208–213.
51. Barrowman, J., Wiley, P.A., Hudon-Miller, S.E., Hrycyna, C.A. and Michaelis, S. (2012) Human ZMPSTE24 disease mutations: residual proteolytic activity correlates with disease severity. *Hum. Mol. Genet.*, **21**, 4084–4093.
52. Saleem, M.A., Zavadil, J., Bailly, M., McGee, K., Witherden, I.R., Pavenstadt, H., Hsu, H., Sanday, J., Satchell, S.C., Lennon, R., et al. (2008) The molecular and functional phenotype of glomerular podocytes reveals key features of contractile smooth muscle cells. *Am. J. Physiol. Renal Physiol.*, **295**, F959–F970.
53. Wang, L., Ellis, M.J., Gomez, J.A., Eisner, W., Fennell, W., Howell, D.N., Ruiz, P., Fields, T.A. and Spurney, R.F. (2012) Mechanisms of the proteinuria induced by Rho GTPases. *Kidney Int.*, **81**, 1075–1085.
54. Schell, C., Baumhagl, L., Salou, S., Conzelmann, A.C., Meyer, C., Helmstadter, M., Wrede, C., Grahmmer, F., Eimer, S., Kerjaschki, D., et al. (2013) N-wasp is required for stabilization of podocyte foot processes. *J. Am. Soc. Nephrol.*, **24**, 713–721.
55. Lopez, L.C., Schuelke, M., Quinzii, C.M., Kanki, T., Rodenburg, R.J., Naini, A., Dimauro, S. and Hirano, M. (2006) Leigh syndrome with nephropathy and CoQ10 deficiency due to decaprenyl diphosphate synthase subunit 2 (PDSS2) mutations. *Am. J. Hum. Genet.*, **79**, 1125–1129.
56. Diomedes-Camassei, F., Di Giandomenico, S., Santorelli, F.M., Caridi, G., Piemonte, F., Montini, G., Ghiggeri, G.M., Murer, L., Barisoni, L., Pastore, A., et al. (2007) COQ2 nephropathy: a newly described inherited mitochondrialopathy with primary renal involvement. *J. Am. Soc. Nephrol.*, **18**, 2773–2780.
57. Quinzii, C.M., Lopez, L.C., Gilkerson, R.W., Dorado, B., Coku, J., Naini, A.B., Lagier-Tourenne, C., Schuelke, M., Salviati, L., Carozzo, R., et al. (2010) Reactive oxygen species, oxidative stress, and cell death correlate with level of CoQ10 deficiency. *Faseb J.*, **24**, 3733–3743.
58. Ozaltin, F. (2014) Primary coenzyme Q10 (CoQ10) deficiencies and related nephropathies. *Pediatr. Nephrol.*, **29**, 961–969.
59. Gast, C., Pengelly, R.J., Lyon, M., Bunyan, D.J., Seaby, E.G., Graham, N., Venkat-Raman, G. and Ennis, S. (2016) Collagen (COL4A) mutations are the most frequent mutations

- underlying adult focal segmental glomerulosclerosis. *Nephrol. Dial. Transplant*, **31**, 961–970.
60. He, Y., Balasubramanian, M., Humphreys, N., Waruiru, C., Brauner, M., Kohlhase, J., O'Reilly, R. and Has, C. (2016) Intronic ITGA3 Mutation Impacts Splicing Regulation and Causes Interstitial Lung Disease, Nephrotic Syndrome, and Epidermolysis Bullosa. *J. Invest. Dermatol.*, **136**, 1056–1059.
61. Boyer, O., Woerner, S., Yang, F., Oakeley, E.J., Linghu, B., Gribouval, O., Tete, M.J., Duca, J.S., Klickstein, L., Damask, A.J., et al. (2013) LMX1B mutations cause hereditary FSGS without extrarenal involvement. *J. Am. Soc. Nephrol.*, **24**, 1216–1222.
62. Konomoto, T., Imamura, H., Orita, M., Tanaka, E., Moritake, H., Sato, Y., Fujimoto, S., Harita, Y., Hisano, S., Yoshiura, K., et al. (2016) Clinical and histological findings of autosomal dominant renal-limited disease with LMX1B mutation. *Nephrology*, **21**, 765–773.
63. Han, Z. and Olson, E.N. (2005) Hand is a direct target of Tinman and GATA factors during *Drosophila* cardiogenesis and hematopoiesis. *Development*, **132**, 3525–3536.